Analyst

PAPER

View Article Online
View Journal

Cite this: DOI: 10.1039/c5an00008d

N-doped TiO_2 based visible light activated label-free photoelectrochemical biosensor for detection of Hg^{2+} through quenching of photogenerated electrons†

Qianqian Han,‡[a,b] Kewei Wang,‡[a] Lijun Xu,[a] Xiang Yan,[a] Kunchi Zhang,[a] Xing Chen,[a] Qinglin Wang,[a] Lan Zhang[b] and Renjun Pei*[a]

Received 4th January 2015,
Accepted 7th April 2015

DOI: 10.1039/c5an00008d

www.rsc.org/analyst

A novel photoelectrochemical (PEC) biosensor was fabricated based on N-doped TiO_2 for the detection of Hg^{2+} through the quenching of photogenerated electrons. The N-doped TiO_2 was synthesized by a sol–gel method with urea and tetrabutyl titanate as the N and Ti sources. Compared with the undoped TiO_2, the N-doped TiO_2 showed an enhanced photocurrent response under visible light (λ > 420 nm). The sensing surface was functionalized with 5′-amino-modified T-rich oligonucleotides. The photoelectrochemical biosensor bound Hg^{2+} on the surface by a highly specific T–Hg^{2+}–T recognition. Hg^{2+} on the surface of the N-doped TiO_2 film withdrew the photogenerated electrons and decreased the recorded current signal. The dynamic linear range for Hg^{2+} has been determined to be as low as 2–6 μM.

Introduction

Photoelectrochemical (PEC) sensors are a new branch of electrochemical detection methods and have the advantages of simple and convenient properties. A light source excites the PEC sensor to generate electron–hole pairs; the electrons are transferred to the conducting substrate, while the holes react with the electron donors at the surface of the solution.[1,2] In these PEC devices, the detection system introduces only a low background signal by utilizing two relatively independent processes: light as an activating source and the current as the detection signal.[3–6]

For a PEC sensor, one of the most important aspects is the selection of a suitable photoelectric semiconductor material; a series of semiconductors have been reported to construct the photo-active layers, such as TiO_2,[7,8] ZnO[9] and CdS.[10] TiO_2 is the most popular material in photoelectrochemical applications due to its low cost and non-toxicity. However, TiO_2 is a wide bandgap semiconductor, with a bandgap around 3.2 eV for the anatase phase, indicating that it cannot absorb in the visible region of the electromagnetic spectrum that constitutes the major fraction of solar radiation and commercial light sources. In order to improve the photoelectric conversion efficiency, some modification methods have been reported, such as doping and deposition.[11] The reported deposition methods commonly use Cd series quantum dots,[12] noble metals[13,14] or dyes.[15] They are good sensitizers for the enhancement of visible light adsorption. However, quantum dots contain a toxic heavy metal and are at risk of photocorrosion. Noble metals and dyes are usually expensive. Moreover, for organic dyes, complex chemical coupling is needed to prevent detachment, and long-term stability is questionable due to photodegradation. Doping introduces foreign atoms into the original crystal lattice and can shift the absorption edge of TiO_2 to a higher wavelength with high photo- and chemical stability. It is also very simple to prepare doped TiO_2 electrodes for the enhancement of visible light absorption. Nitrogen doping has proven indispensable for band-gap narrowing and photoelectrochemical activity compared with other atoms.[16] However, N-doped TiO_2 photoelectrochemical biosensors have not been reported, except in the form of (N,F)-codoped TiO_2 nanotubes for the study of acetylcholinesterase inhibition induced by endogenous neurotoxins[17] and in the application of electrochemiluminescence for adenosine analysis.[18]

[a]Key Laboratory of Nano-Bio Interface, Division of Nanobiomedicine, Collaborative Innovation Center of Suzhou Nano Science and Technology, Suzhou Institute of Nano-Tech and Nano-Bionics, Chinese Academy of Sciences, Suzhou, 215123, China. E-mail: rjpei2011@sinano.ac.cn
[b]School of Materials Science and Engineering, Xi'an Jiaotong University, Xi'an, 710049, China

†Electronic supplementary information (ESI) available. See DOI: 10.1039/c5an00008d

‡The two authors contributed equally to this work.

In order to introduce the N-doped TiO_2 material into the PEC biosensor system, the choice of a highly sensitive and selective recognition system is another important aspect. T–Hg^{2+}–T recognition has attracted significant interest due to its high selectivity, strong binding and environmental applications. Mercury (Hg) is widely regarded as an extremely toxic pollutant that can affect the immune system, alter genetic and enzyme systems, and damage the nervous system, including coordination and the senses of touch, taste, and sight. Although inductively coupled plasma mass spectrometry (ICP-MS) is commonly used to detect Hg, the expense of such systems and their complex properties limit the technique's application, especially in the outside environment. Therefore, a low cost, lightweight, sensitive and selective detection method is required. The detection of Hg usually involves chemical transformation of the elemental form to Hg^{2+}, which is water soluble and can easily react with a chelator or other reagents. Under these conditions, Hg^{2+} is found to have a special affinity with thymine to form a stable T–Hg^{2+}–T complex,[19] which is even more stable than the common A–T pair in DNA double strands.[20] Hg^{2+} detection based on the T–T pair has been extensively explored.[21–24] Interestingly, Freeman has utilized T–Hg^{2+}–T complexing to quench the luminescence of CdSe/ZnS QDs by binding Hg^{2+}.[25] This impels us to design a novel T–Hg^{2+}–T-based photoelectrochemical approach to sense Hg^{2+} through quenching of photogenerated electrons by Hg^{2+}, using the electron-withdrawing properties of Hg^{2+}. Meanwhile, the form of the T–Hg^{2+}–T structure can easily cause a single DNA strand to change conformation into a double strand[26–28] or hairpin structure.[23] Several photoelectrochemical sensors have been developed for Hg^{2+} detection based on the T–Hg^{2+}–T interaction. In these studies, the formation of DNA double strands or hairpin structures due to Hg^{2+} binding can change the amount of the photocurrent enhancer, which could be a quercetin–copper(II) complex, nano-gold, $Ru(bpy)_2(dppz)^{2+}$, or CdS QDs, on the PEC interface.[27–30]

In this study, we fabricated a T–Hg^{2+}–T-based PEC biosensor on an N-doped TiO_2 electrode for the detection of Hg^{2+} through the quenching of photogenerated electrons. The T-rich species was immobilized on the hydroxylated surface of N-doped TiO_2 by (3-aminopropyl)triethoxysilane (APTES) and glutaraldehyde (GA). Multiple Hg^{2+} ions from the buffer solution adsorbed on to the T-rich strand through the highly selective T–Hg^{2+}–T interaction, and an obviously decreased photocurrent signal was observed due to the electron withdrawing effect of the bound Hg^{2+}. The results revealed that the visible light activated PEC sensor was suitable for detection of trace concentrations of Hg^{2+} ions through the sensitive and specific T–Hg^{2+}–T interaction and that the sensor would greatly benefit environmental monitoring.

Experimental

Reagents and instruments

Tetrabutyl titanate was purchased from Sinopharm Chemical Reagent Corporation Ltd. All other chemicals were of analytical grade and were used as received without further purification. Tris(hydroxymethyl)aminomethane–HNO_3 buffer solution (10 mM Tris-HNO_3, pH = 7.4) was prepared by adjusting the pH value of a 10 mM Tris solution to 7.4 with diluted nitric acid. Phosphate buffer solution (PBS, 0.1 M) was prepared by mixing 0.1 M Na_2HPO_4 and 0.1 M KH_2PO_4 solutions to pH 7.4. All solutions were prepared using Milli-Q pure water.

The oligonucleotides were synthesized and purified by Invitrogen Biotechnology. The 5′ end of the two sequences were modified by NH_2 groups as follows:

QT1, 5′-NH_2-TTGTTGTTCCCCTTCTTCTT;

QC2, 5′-NH_2-CCTCCTTCCTTCAAAACAACCAACCACC.

The photoelectrochemical detection experiments were carried out at room temperature with a CHI660D electrochemical system (CH Instruments). Scanning electron microscopic (SEM) images were recorded by a Quanta 400F instrument (FEI). The structure of the prepared TiO_2 and N-doped TiO_2 crystal powders were analyzed by an ARL X'TRA X-ray diffraction instrument (American Thermo Elemental Company), with monochromatized Cu Kα radiation (λ = 1.5418 Å). UV-vis diffuse reflectance spectra were recorded by a Jasco V-660 instrument (Jasco Ltd, Japan).

Preparation of the biosensor

Methods for preparation of the N-doped TiO_2 powder and film, as well as the morphologies and the XRD patterns (Fig. S1), are in the ESI.†

The N-doped TiO_2/FTO electrode was illuminated with a Xe lamp for 30 min in the presence of several drops of water. The electrode was then immersed in a 1% APTES–ethanol solution for 30 min, and washed with ethanol and water respectively. After that, the electrode was transferred into a 2.5% GA solution (10 mM PBS, pH = 7.4) for 1 h and completely washed with water. Then the T-rich DNA was diluted to 5 μM with pure water, and the mixture of 4 μL DNA and 16 μL PBS was dropped onto the GA-modified electrode. After reacting for 12 h, the electrode was carefully rinsed with 10 mM Tris-HNO_3 (pH = 7.4) to remove the adsorbed DNA.

Photoelectrochemical determination

A three electrode system, comprising the modified N-TiO_2/FTO glass as the working electrode, a platinum foil as the auxiliary electrode and an Ag/AgCl electrode as reference electrode, was employed for all photoelectrochemical experiments. The electrolyte was 10 mM Tris-HNO_3 (pH = 7.4) and the *i–t* curve method was used to obtain the photocurrent responses with a potential of 0 V. A 500 W Xe lamp (80 mW cm^{-2}) was used as the light source and was equipped with a UV cut-off filter (λ > 420 nm). During the photoelectrochemical testing, the test area of the working electrode was confined to 0.25 cm^2 by sealing with Silastic. After the background photocurrent stabilized, the photocurrent response was subsequently recorded as the excitation light was turned on and off.

Results and discussion

Design strategy of the photoelectrochemical biosensor

The amino labeled T-rich species, QT1, was chosen as a recognition element and a layer of visible light sensitive N-doped TiO_2 film was chosen as a transducer to fabricate the photoelectrochemical biosensor. The detection method procedure is described in Scheme 1. Initially, the single strand T-rich DNA exhibited an open conformation in the detection buffer (10 mM Tris-HNO_3, pH = 7.4), which presented as a high photocurrent response from the illuminated N-doped TiO_2. In this process, the N-doped TiO_2 film absorbed the visible light energy and electrons were excited into the conduction band, while the holes remained near the valence band. After that, the electrons flowed into the conductive glass, and the holes were annihilated by donated electrons at the electrode–solution interface. The photocurrent response was recorded and found to be dependent on the photovoltaic properties of the semiconductor. In the presence of Hg^{2+}, the T-rich DNA folded into a conformationally restricted hairpin structure capturing and thereby recognizing the ions. Furthermore, the photo-generated electrons were more likely to transfer to the bound Hg^{2+} due to the electron-withdrawing properties of Hg^{2+}. Within a certain range, a decreased photocurrent response was obtained following an increase in the concentration of Hg^{2+}. The photocurrent responses for the fabrication process of the PEC biosensor are shown in Fig. S2.† This fabrication strategy is the first to apply the withdrawing effect of Hg^{2+} to a PEC biosensor, which showed a correspondingly fast response speed.

The enhanced visible light adsorption and photo-response of the N-doped TiO_2

The diffuse reflectance spectra of both the undoped TiO_2 and N-doped TiO_2 are shown in Fig. 1A to demonstrate the enhanced light absorption in the case of N-doping. The absorption edge of undoped TiO_2 was about 380 nm, corresponding to the band gap of anatase (3.2 eV), indicating that it only absorbed high energy light in the ultraviolet range. However, illumination by ultraviolet light is often harmful to common bio-systems, so an improvement to maximize light absorption was needed. Compared with the diffuse reflectance spectrum of undoped TiO_2, that of the N-doped TiO_2 showed an obvious red-shift inclined edge from 400 nm to around 600 nm in the visible light region. This showed that the N-doping method efficiently enlarged the crystal lattice and narrowed the band gap of TiO_2, which could then be excited under visible light to promote the generation of a photocurrent.

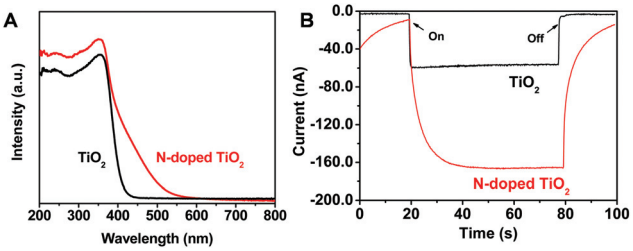

Fig. 1 Diffuse reflectance spectra (A) and the photocurrent responses (B) of TiO_2 and N-doped TiO_2.

The corresponding photoelectrochemical responses of the undoped TiO_2 and N-doped TiO_2 were investigated under the illumination of a Xe lamp with a UV cut-off filter ($\lambda > 420$ nm). Under these conditions, illumination of pure TiO_2 resulted in a weak photocurrent as shown in Fig. 1B. Meanwhile, the photocurrent of N-doped TiO_2 electrode was triple that of the undoped TiO_2 due to the visible light absorption. The photocurrent of N-doped TiO_2 can be expected to further increase by controllably preparing doped TiO_2 nanomaterials with better visible light adsorption. Moreover, the photocurrent responses of the two electrodes were unstable in the first off–on cycle because of the unbalanced recombination status between the excited electrons and holes. The photocurrents stabilized in the second 30 s, so a 60 s light-on period was chosen in the experiment.

Photocurrent response of the photoelectrochemical biosensor in the presence of Hg^{2+}

The detection of Hg^{2+} was performed using T-rich DNA (QT1) immobilized on an N-doped TiO_2 electrode in buffer solution (10 mM Tris-HNO_3, pH = 7.4). The photocurrent curves were recorded before and after the electrode was incubated at room temperature for 30 min with different concentrations of Hg^{2+}. Under visible light illumination ($\lambda > 420$ nm), it was found that the photocurrent intensities decreased with increasing Hg^{2+} concentration. Fig. 2A depicts the concentration dependent photocurrent intensity curves upon interaction with QT1 in the presence of 1–7 μM Hg^{2+}, at last showing that the decreased photocurrent intensity reached a steady state. Fig. 2B shows the derived calibration curve corresponding to the photocurrent signal decreases at each concentration ($\Delta I = I - I_0$). Here I_0 is the photocurrent from the DNA immobilized N-doped TiO_2 in the absence of Hg^{2+}, and I is the photocurrent after the electrode was incubated with Hg^{2+}. A linear response

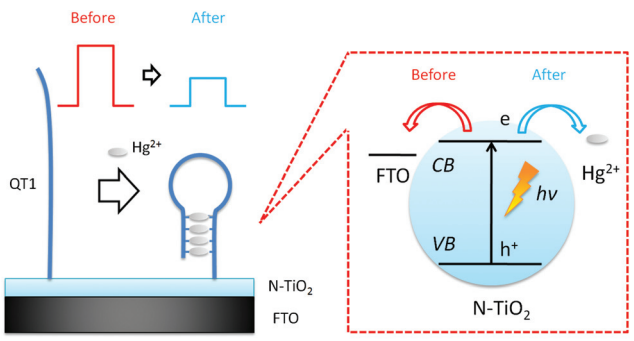

Scheme 1 The schematic illustration of the transformation of QT1 (left) and the mechanism of the electron transfer routes (right) before and after the binding of Hg^{2+}.

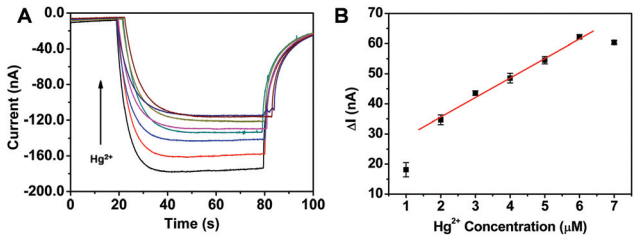

Fig. 2 (A) Photoelectrochemical responses of the DNA/N-doped TiO_2 electrode before and after incubating with concentrations of Hg^{2+} ranging from 1 to 7 μM for 30 min. The arrow shows the increasing Hg^{2+} concentrations. (B) The calibration curve of the photocurrent responses for various concentrations of Hg^{2+}.

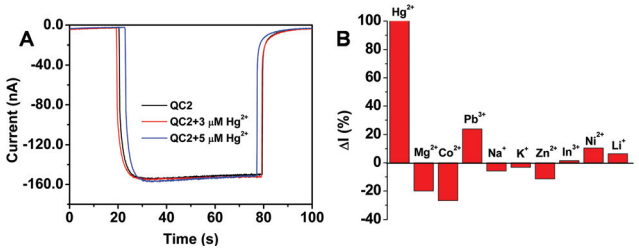

Fig. 3 (A) Photoelectrochemical response of the QC2 species after reaction with 3 μM and 7 μM Hg^{2+} following a 30 min incubation. (B) Selectivity of the analysis of Hg^{2+} by QT1. The concentrations of all metal ions were 10 μM.

was found in the range of 2–6 μM Hg^{2+} and the detection limit was 0.40 μM. When the concentration exceeded 7 μM, the photocurrent response reached a plateau, indicating saturation of the sites available to bind Hg^{2+}.

Selectivity of the photoelectrochemical biosensor

Control experiments revealed that decreases of photocurrent occurred due to the reaction between Hg^{2+} and thymines. As shown in Fig. 3A, a C-rich species of QC2 was chosen as a control strand. The photocurrent responses of the immobilized QC2 before and after Hg^{2+} addition exhibited nearly the same value, indicating that the structure of QC2 prevented the formation of T–Hg^{2+}–T complexes to capture Hg^{2+}.

Fig. 3B shows the ion selectivity of the QT1 modified N-doped TiO_2 electrode in the presence of some common metal ions. The photocurrent responses were recorded in the presence of each type of metal ion respectively, at a concentration of 10 μM in 10 mM Tris-HNO_3 (pH = 7.4). These ions had little effect on the change of photocurrent responses compared with the maximum photocurrent decrease of Hg^{2+}, indicating a high specificity of the proposed photoelectrochemical biosensor.

Conclusions

In summary, a highly sensitive and selective N-doped TiO_2 based photoelectrochemical biosensor was fabricated for the determination of Hg^{2+} concentration through the quenching of photogenerated electrons. The photoelectrochemical biosensor bound Hg^{2+} on the surface by utilizing a highly specific T–Hg^{2+}–T recognition. The electrode of the N-doped TiO_2 showed an enhanced photocurrent response under visible light compared with the undoped TiO_2 electrode. With the introduction of N-doped TiO_2, a concentration as low as 0.4 μM of Hg^{2+} could be detected in aqueous solution. Furthermore, this method avoids additional labeling, leading to a low cost and convenient application. Considering the advantages of the N-doped TiO_2 based photoelectrochemical biosensor through the quenching of photogenerated electrons, we expect this sensor to be a useful tool for the detection of analytes in the environment and living systems.

Acknowledgements

This work was financially supported by the Natural Science Foundation of Jiangsu Province (BK20130349) and the National Natural Science Foundation of China (no. 21275156, 31301495).

Notes and references

1 W. W. Zhao, J. J. Xu and H. Y. Chen, *Chem. Rev.*, 2014, **114**, 7421–7441.
2 W. Yao, A. L. Goff, N. Spinelli, M. Holzinger, G. W. Diao, D. Shan, E. Defrancq and S. Cosnier, *Biosens. Bioelectron.*, 2013, **42**, 556–562.
3 X. R. Zhang, M. S. Liu, H. X. Liu and S. S. Zhang, *Biosens. Bioelectron.*, 2014, **56**, 307–312.
4 X. R. Zhang, Y. S. Guo, M. S. Liu and S. S. Zhang, *RSC Adv.*, 2013, **3**, 2846–2857.
5 Z. Yue, F. Lisdat, W. J. Parak, S. G. Hickey, L. Tu, N. Sabir, D. Dorfs and N. C. Bigall, *ACS Appl. Mater. Interfaces*, 2013, **5**, 2800–2814.
6 R. Freeman, J. Girsh and I. Willner, *ACS Appl. Mater. Interfaces*, 2013, **5**, 2815–2834.
7 W. W. Zhao, Z. Y. Ma, J. J. Xu and H. Y. Chen, *Anal. Chem.*, 2013, **85**, 8503–8506.
8 H. B. Li, J. Li, W. Wang, Z. J. Yang, Q. Xu and X. Y. Hu, *Analyst*, 2013, **138**, 1167–1173.
9 L. Xia, J. Song, R. Xu, D. L. Liu, B. Dong, L. Xu and H. W. Song, *Biosens. Bioelectron.*, 2014, **59**, 350–357.
10 X. Y. Zhang, F. Xu, B. Q. Zhao, X. Ji, Y. W. Yao, D. P. Wu, Z. Y. Gao and K. Jiang, *Electrochim. Acta*, 2014, **133**, 615–622.
11 X. B. Chen and S. S. Mao, *Chem. Rev.*, 2007, **107**, 2891–2959.
12 M. Zheng, Y. Cui, X. Y. Li, S. Q. Liu and Z. Y. Tang, *J. Electroanal. Chem.*, 2011, **656**, 167–173.
13 G. H. Chen, J. L. Wang, C. Y. Wu, C. Z. Li, H. Jiang and X. M. Wang, *Langmuir*, 2012, **28**, 12393–12399.

14 P. P. Wang, W. J. Dai, L. Ge, M. Yan, S. G. Ge and J. H. Yu, *Analyst*, 2013, **138**, 939–945.
15 J. Tang, B. Kong, Y. C. Wang, M. Xu, Y. L. Wang, H. Wu and G. G. Zheng, *Nano Lett.*, 2013, **13**, 5350–5354.
16 R. Asahi, T. Moikawa, T. Ohwaki, K. Aoki and Y. Taga, *Science*, 2001, **293**, 269–271.
17 Q. L. Huang, H. Chen, L. L. Xu, D. Q. Lu, L. L. Tang, L. T. Jin, Z. A. Xu and W. Zhang, *Biosens. Bioelectron.*, 2013, **45**, 292–299.
18 C. Y. Tian, J. J. Xu and H. Y. Chen, *Chem. Commun.*, 2012, **48**, 8234–8236.
19 Y. Tanaka, S. Oda, H. Yamaguchi, Y. Kondo, C. Kojima and A. Ono, *J. Am. Chem. Soc.*, 2006, **129**, 244–245.
20 Y. Miyake, H. Togashi, M. Tashiro, H. Yamaguchi, S. Oda, M. Kudo, Y. Tanaka, Y. Kondo, R. Sawa, T. Fujimoto, T. Machinami and A. Ono, *J. Am. Chem. Soc.*, 2006, **128**, 2172–2173.
21 A. Ono and H. Togashi, *Angew. Chem., Int. Ed.*, 2004, **43**, 4300–4302.
22 X. J. Xue, F. Wang and X. G. Liu, *J. Am. Chem. Soc.*, 2008, **130**, 3244–3245.
23 Z. Q. Zhu, Y. Y. Su, J. Li, D. Li, J. Zhang, S. P. Song, Y. Zhao, G. X. Li and C. H. Fan, *Anal. Chem.*, 2009, **81**, 7660–7666.
24 T. Li, S. J. Dong and E. K. Wang, *Anal. Chem.*, 2009, **81**, 2144–2149.
25 R. Freeman, T. Finder and I. Willner, *Angew. Chem., Int. Ed.*, 2009, **48**, 7818–7821.
26 S. J. Liu, J. H. Jiang, G. L. Shen and R. Q. Yu, *Anal. Chem.*, 2009, **81**, 5724–5730.
27 H. B. Li, Y. Xue and W. Wang, *Biosens. Bioelectron.*, 2014, **54**, 317–322.
28 J. Li, W. W. Tu, H. B. Li, M. Han, Y. Q. Lan, Z. H. Dai and J. C. Bao, *Anal. Chem.*, 2014, **86**, 1306–1312.
29 B. T. Zhang and L. H. Guo, *Biosens. Bioelectron.*, 2012, **37**, 112–115.
30 Z. Y. Ma, J. B. Pan, C. Y. Lu, W. W. Zhao, J. J. Xu and H. Y. Chen, *Chem. Commun.*, 2014, **50**, 12088–12090.